Journal of Alloys and Compounds 510 (2012) 26–32

Contents lists available at SciVerse ScienceDirect

Journal of Alloys and Compounds

journal homepage: www.elsevier.com/locate/jallcom

Review

Effect of extrusion ratio on the wear behaviour of Al–Si and Al–Mg alloys

H.İ. Demirci*, H. Evlen

Karabuk University Faculty of Technical Education, Department of Mechanical Education, 78050 Karabuk, Turkey

ARTICLE INFO

Article history:
Received 19 February 2010
Received in revised form 19 August 2011
Accepted 22 August 2011
Available online 27 August 2011

Keywords:
Al–Mg alloy
Al–Si alloy
Hot extrusion
Wear

ABSTRACT

In this study, the wear behaviour of hot extruded Al–Si and Al–Mg alloys was investigated under dry conditions. Die cast Al–Mg alloy containing 1.7% Mg and Al–Si alloy containing 3.3% Si were extruded at 1.6 and 2 ratios. Mechanical and microstructural characterisations of the extruded alloys were carried out through optical microscopy, hardness measurements and tensile testing. Wear tests were carried out on a pin-on-disc type wear device and the worn surfaces were examined under a scanning electron microscope (SEM). The wear test results revealed that the extrusion ratio had an influence on the wear rate and that the samples extruded at a ratio of 1.6 had a lower wear resistance than the ones extruded at a ratio of 2.

Contents

1. Introduction

There is a growing interest in the wear behaviour of aluminium alloys as more and more of these alloys, both in type and quantity, are being used in different areas of technology [1,2]. Of the aluminium-based alloys, aluminium–silicon alloys are probably the most investigated ones for their tribological behaviour [3–8]. In recent years, aluminium–magnesium alloys have been very attractive in the applications for the automotive, railway and aerospace industries from an ecological point of view. One of the technical attractions for the widespread use of magnesium alloys in structural applications is the improvement of creep strength at elevated temperatures [9–16]. Aluminium–silicon alloys have drawn a great deal of attention from the automotive industry, device and machine manufacturing, construction and architecture since they have very good mechanical and physical properties, good formability, high strength, superior corrosion resistance, good wear features and weldability [17,18]. Various researchers have long been studying the shaping of aluminium alloys using extrusion.

The hydraulic extrusion press was invented in 1810 by an Englishman called S. Bramah. His press was designed for the extrusion of lead. The first successful application of the process was on alloys with high melting points, applied by a German called A. Dick, in the 1890s [19,20]. Extrusion is a deformation process used to produce long, straight, semi-finished metal products such as bars, solid and hollow sections, tubes, wires and strips. The principle of the process is that; under high load, a billet is squeezed from a closed container through a die to give a reduction in size [19]. Cross sections of varying complexity can be extruded at a room temperature, or at high temperatures, depending on the dies, the alloy and the method used.

Extrusion ratio (ER) [20] of a die is

$$E_R = \frac{A_c}{n \times (A_E)}$$

where "n" is the number of symmetrical parts, "A_c" is the cross-sectional area of the billet to be extruded and "A_E" is the cross

* Corresponding author. Tel.: +90 370 433 82 00x1055; fax: +90 370 433 82 04.
E-mail addresses: hdemirci@karabuk.edu.tr, hietybdemirci@hotmail.com (H.İ. Demirci).

0925-8388/$ – see front matter © 2011 Elsevier B.V. All rights reserved.
doi:10.1016/j.jallcom.2011.08.074

Table 1
Extrusion processing conditions for extrusion ratios of 1.6 and 2.

Parameter	Ext. ratio 1.6	Ext. ratio 2
Mat. input temp.	350 ± 5 °C	350 ± 5 °C
Die input temp.	300 ± 5 °C	300 ± 5 °C
Sample input dia.	20 mm	20 mm
Sample output dia.	16 mm	14 mm
Sample input leng.	50 mm	50 mm
Sample output leng.	70 mm	100 mm
Sample output temp.	128 °C	135 °C
Sample exit time	50 s	55 s
Press pressure	2.5–3 MPa	2.5–3 MPa

sectional area of the extruded-product. In this study only one part at a time is extruded, therefore $n = 1$, A_C is constant, and accordingly when the extrusion ratio of a profile is low, A_E is high.

The extrusion ratio of a shape is a direct indicator of the mechanical energy used while obtaining the shape with extrusion.

It is clear from the published work that there are various studies regarding the effects of the extrusion ratio on the mechanical and wear behaviour of aluminium alloys [21–25]. In the previous studies, experiments were carried out for extrusion ratios reaching up to 40; their results showed that after the extrusion procedure, a 70–80% deformation occurred [26–28]. The structure of aluminium subjected to low ratios of extrusion is similar to that of the cast aluminium (coarse-grained). This structure is mechanically weak. Hence, it is likely that mechanical and physical properties of the products subjected to extrusion at the ratios below 10 may vary from the values reported in the literature [20]. In addition, some investigations show that a higher extrusion ratio (≥39) is more effective than a lower one (≤24) to refine the grains for Mg alloys [25]. Milenin et al. [29] conducted studies with an extrusion ratio of 5. After analysing the results of the extruded sample, the procedure was regarded as successful. This is the lowest extrusion ratio in the literature.

In this study, Mg and Si in a similar amount to the Si and Mg contents of commercial aluminium alloys were added to form a binary alloy and the effects of the alloying elements were analysed. Al–Si and Al–Mg alloys were produced using die casting. The produced samples were extruded using various extrusion ratios that were lower than 5, 1.6 and 2. Standard characterisation procedures were applied to the extruded samples and microstructure images were taken. Microhardness measurements and the tensile test were conducted on the samples.

2. Experimental procedures

In this study, Al–Mg alloys, with a chemical composition of 1.7% Mg, 0.6% Si, 0.3% and Al–Si alloys with a chemical composition of 3.3% Si, 0.41% Mg, 0.585% were produced using die casting method in the dimensions of Ø20 mm × 150 mm. The casting temperature of the analysed alloys was determined as 720 °C, using a chromel–alumel thermocouple. The metal mould was pre-heated at 220 °C, prior to the casting procedure. After the casting process, Al–Mg alloys were homogenised for an hour at 400 °C, while Al–Si alloys were homogenised for an hour at 500 °C, in order to avoid segregations. The homogenised samples were cut to Ø20 mm × 50 mm dimensions for extrusion. The extrusion was carried out under the experimental conditions indicated in Table 1, with the help of a 50-ton hydraulic press, at two different ratios (1.6 and 2). While the input temperature of the materials was 350 °C, the die input temperature was 300 °C and input diameter was 20 mm for all the samples. Pre-prepared dies with 2° and 3° draft angles were used.

The extruded samples were subjected to microstructural characterisation, grain size measurements, microhardness measurements, tensile test and wear tests. Standard procedures were used for microstructural characterisation. Optical microscopy analysis and scanning electron microscopy (SEM) analysis were conducted at this stage. The samples were then cold mounted using a PRESI mounting kit in order to conduct metallographic examinations. All samples were ground using a PRESI MECAPOL P262 device with 180, 240, 320, 600 and 1200 grits emery papers. Polishing was carried out using a 3 μm and 1 μm diamond solution. After being polished with 1 μm, the samples were cleaned using pure alcohol and etched for 10 s with 2.5 ml HNO_3, 1.5 ml HCl, 1 ml HF, 95 ml H_2O. Microstructural analysis of the polished samples was carried out using a MEIJI ML 7100 optical microscope. Moreover, SEM images for micro-structural studies were obtained using a JEOL JSM 6060 model device. Grain size measurements of the extruded samples (vertical and parallel to the extrusion direction) were conducted using the MSQ Plus Image Analysis System according to ASTM E112.

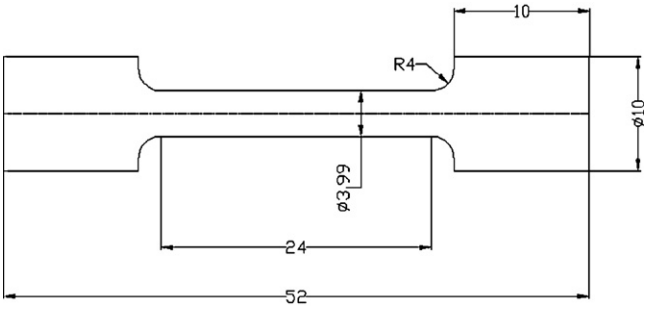

Fig. 1. Dimensions of the tensile test sample.

In addition, micro-hardness measurements of the extruded samples were carried out using an HMV-2 SHIMADZU microhardness measuring device with a measurement precision of ±0.01 μm. The load applied during hardness measurements was 50 g and the period of the application was 10 s. The mean of five measurements was taken for each sample. The tensile test was applied to the Al–Si and Al–Mg alloys using a 20 kN-capacity ZWICK tensile testing device. The tensile test was conducted at a tensile speed of 3×10^{-5} m/s. Samples for the tensile test were prepared in accordance with the ASTM E8M standard. Fig. 1 illustrates the dimensions of the tensile samples.

The extruded samples were subjected to wear test using a pin-on-disc type wear device (Fig. 2) at room temperature at a sliding speed of 1 m/s and under 10 N, 20 N and 30 N loads. Wear samples were prepared in cylindrical form with a 10 mm diameter and a 7 mm height. Wear tests were conducted at four different wear distances (300 m, 600 m, 900 m and 1200 m). Acetone was used to clean the wear samples and the disc before the tests. Wear results were assessed depending on the weight loss in the samples and weighed using scales with a 0.1 mg precision before and after the experiment.

The weight losses were assessed by measuring the samples after each 300 m. The counter-material used was AISI 4140 steel with a hardness of 60 HRC. The worn samples were examined using an SEM in order to determine the wear mechanisms of the worn surfaces.

3. Results and discussion

Fig. 3 illustrates the optical microscope images of die cast Al–Si and Al–Mg alloys used in this study. The images illustrate that the microstructures of both the alloys are dendritic. No pores are visible in the microstructure. While the primer α Al grains are surrounded by Al–Si eutectic in the Al–Si alloy, they are also surrounded by Al–Mg eutectics in the Al–Mg alloy.

Fig. 4A and C illustrates the optical microscope images of Al–Mg and Al–Si alloys that are parallel to the extrusion direction and extruded at the ratio of 2, while Fig. 4B and D illustrates the optical microscope images vertical to the extrusion direction. As is seen from the images (Fig. 4), the grains are elongated in the direction of extrusion. The images of the same alloys have been taken vertical to the direction of extrusion (Fig. 4B and D) show the appearance of an equiaxed grain structure. Such a result reveals that the grain

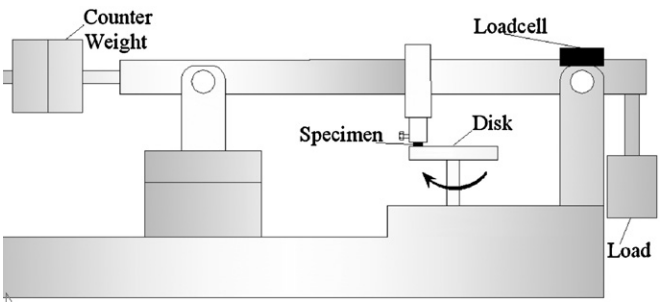

Fig. 2. Pin-on-disc wear test machine.

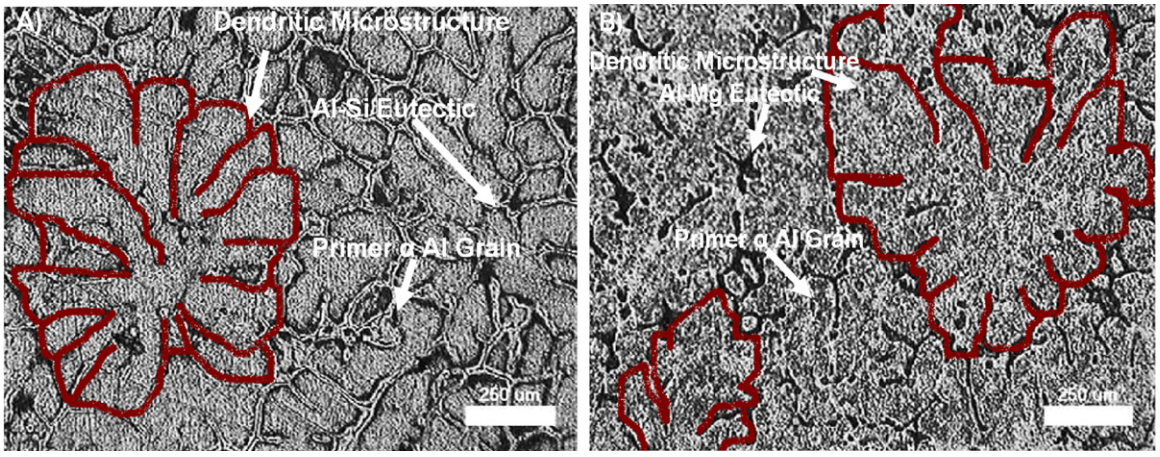

Fig. 3. The optical microscope images of the casting materials: (A) Al–Si alloy and (B) Al–Mg alloy.

structure of the materials undergo a change during the extrusion process. The grain size varies in terms of the extrusion ratio and also re-crystallisation may occur within the structure due to the processing temperature [21,25,30].

As was found in the literature, grains deform in metals under plastic strain and elongate in the direction of the deformation and they become finer with increasing extrusion ratio [31–35]. The density of dislocation increases together with the increase in plastic strain. As dislocation movement becomes difficult due to dislocation entanglement, it is called strain hardening. The dislocation density increases (like a tight spring) as the atoms in the dislocation region move away from their state of equilibrium and ultimately makes the intrinsic energy of the material rise. In that case atoms tend to return to the state of equilibrium that is disrupted. The first thing that happens in the event that external energy (heat) is given to the metal that is exposed to plastic strain is that crystal faults decrease. When the amount of external energy given to the metal is increased, new crystal nuclei will form in the high-energy regions, where the dislocation density is high. As these nuclei grow, the material completes its re-crystallisation process. Just as the crystal grain size of the re-crystallised material depends on the number of nuclei to form and the number of nuclei depends on the abundance of regions where the dislocation density is high, the size of crystal grains depends on the amount of deformation. In the event that the annealing time and temperature of the material is increased, the grains will grow and become large. This is not a desired structure [36].

Zubizarreta et al. [37] compressed two different commercial aluminium powders using a direct hot extrusion method. For the study, the extrusion temperature was 425 °C, and the extrusion ratio was 16:1. Part of the material was sintered at 500 °C before the extrusion process. The variation in the extrusion load and the hardness of the obtained product were constantly examined throughout extrusion. The results showed that samples sintered at 500 °C had a better grain structure. In conclusion, inter-metallic precipitations and re-crystallisation in the structure were observed depending on the process parameters, powder composition, heat behaviour and stresses [37].

Suh et al. [38] investigated the changes in the microstructure of two types of Al–Zn–Mg–Cu–Sc alloys and AA7075 materials after carrying out hot extrusion and subsequent heat treatment processes. Similar to the results of Zubizarreta et al., Suh et al. showed in their study that re-crystallisation occurred in the microstructure of extruded alloys and that recovery continued throughout the heat treatment [37,38]. In conclusion, hardness rapidly increased with the effect of the heat and columnar grains on the sub-surface of the extruded first alloy system and AA7075 alloy; an improvement was observed in the structures due to hot extrusion in the second alloy system. However, re-crystallisation continued during the heat treatment. Increases in grain elongation and hardness were quite low.

Fig. 5 illustrates the values obtained as a result of distance measurements between dendrite arms using the MSQ Plus Image Analysis System. The distance between the dendrite arms was 0.009 mm in 60% of the Al–Si alloy structure and 0.005 mm in 68% of the Al–Mg alloy structure.

Fig. 6 illustrates the grain size measurements obtained from the parallel and vertical cross sections of 1.6 and 2 extruded samples. As is seen from the graphs and tables, the grain size measurements for those parallel to the direction of extrusion are relatively higher than the ones vertical to the direction of extrusion. Upon the comparison of the grain sizes depending on the ratio of extrusion, it is clear that the grain sizes of the samples extruded at the ratio of 2 is larger when compared to the samples extruded at 1.6. That is because the grains are pushed towards the direction of extrusion and elongate to a certain extent through the extrusion process.

Optical microscope images and grain size measurements revealed that thinner and longer grains were obtained in the extruded Al–Si alloy at two different ratios. The addition of Si to Al increases its ductility. When alloyed with magnesium, its strength increases while, formability and ductility properties decrease [21]. It is obvious from the illustrated optical microscope images parallel to the direction of extrusion in Fig. 4A and C that the grains of the Al–Si alloy extruded at the ratio of 2 are elongated more than the ones in the Al–Mg alloy. It proves that Si, as the alloying element, increases its ductility in the aluminium alloy and grains elongate

Table 2
Microhardness values (HMV) for Al–Si and Al–Mg alloys.

Material	1.6 extruded	2 extruded	As-cast	Deviation		
				1.6	2	As-cast
Al–Si	53	51	36	0.6	0.7	2.6
Al–Mg	58	54	65	0.9	1.13	2.1

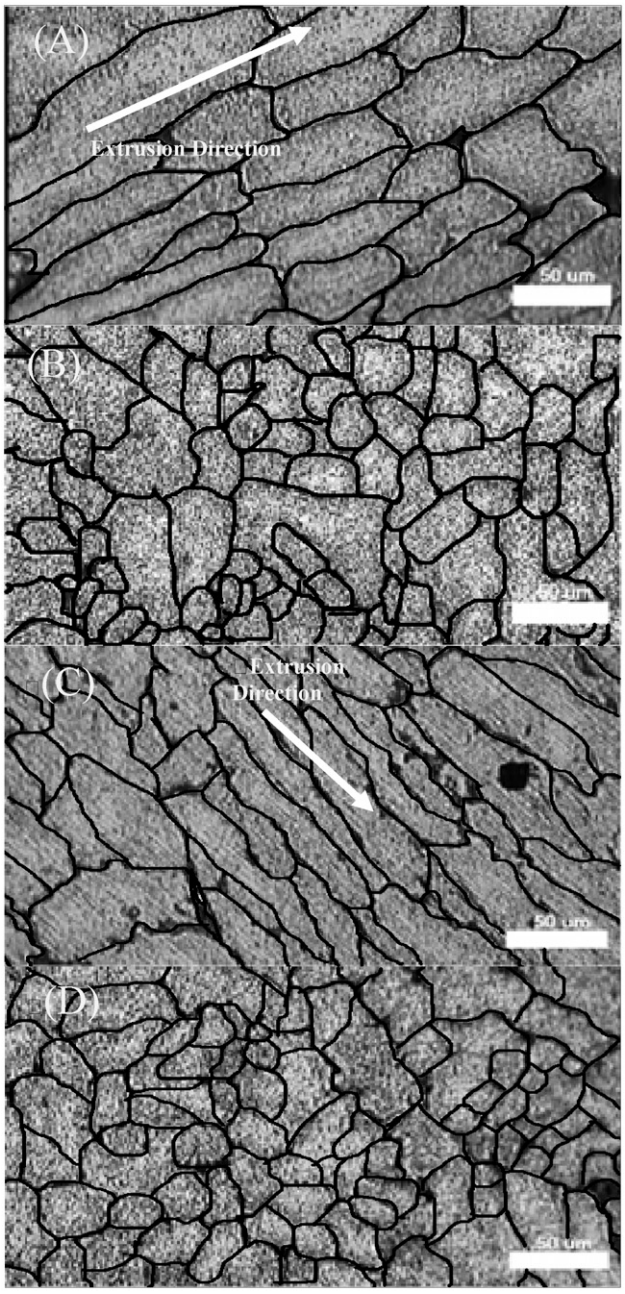

Fig. 4. Optical microscope images for Al–Mg alloys extruded at a ratio of 2: (A) parallel to the direction of extrusion, (B) vertical to the direction of extrusion; optical microscope images for Al–Si alloys extruded at a ratio of 2, (C) parallel to the direction of extrusion, and (D) vertical to the direction of extrusion.

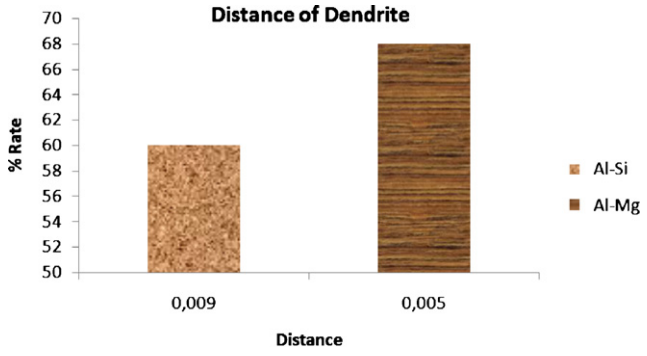

Fig. 5. The distance between dendrite arms.

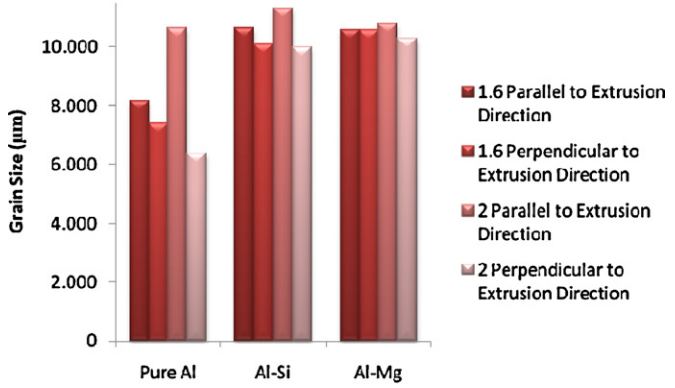

Fig. 6. The grain size in cross sections parallel and vertical to the direction of extrusion.

more; additionally, it is proved that the formability of the Al–Si alloy is better than the Al–Mg alloy [39,8,40].

Table 2 illustrates the results of the microhardness test (HMV) conducted using a 50 g load for as-cast and extruded Al–Si and Al–Mg alloys.

Table 2 illustrates the mean micro-hardness values taken from 10 measurements for each, in HMV, measured from the parallel cross section of 1.6 and 2 extruded alloys. No significant difference was found between the micro-hardness values of 1.6 and 2 extruded samples as both extrusion ratios were low and too close to each other. The microhardness values measured for 1.6 extruded alloys were higher than the micro-hardness values measured for 2 extruded alloys. Microhardness values decrease as the ratio of extrusion increases since the grain structure changes from equiaxed to oblong and the grain elongation increases with the extrusion ratio. It is likely to say that hardness is directly related to

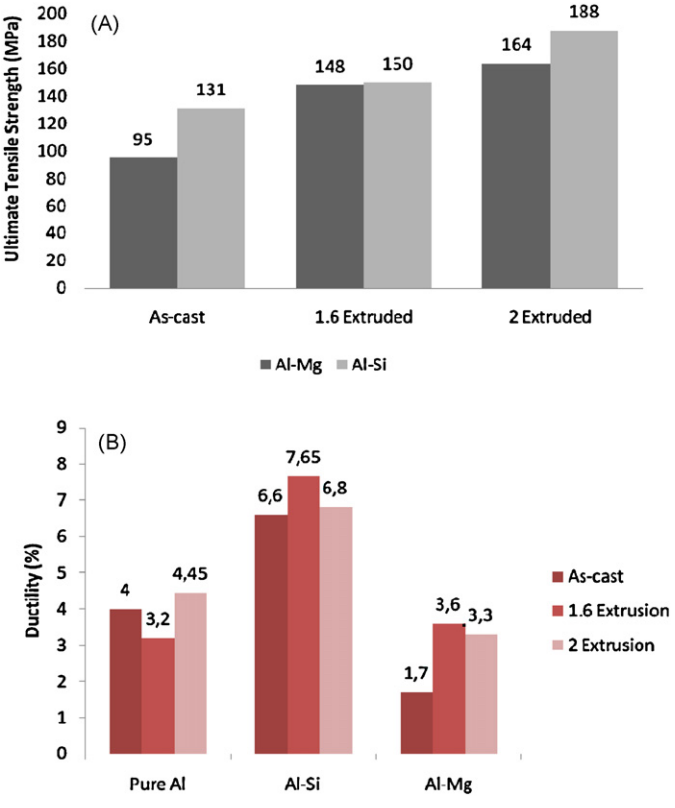

Fig. 7. Tensile test results: (A) ultimate tensile strength and (B) ductility.

grain size. The hardness values of the as-cast samples of the Al–Mg alloy are higher than those of the extruded alloy. Higher hardness of the as-cast samples can be explained by rapid cooling in a metal die. That is because the extruded samples were left to cooling in air while the as-cast samples were left to cooling in a metal die. As the metal die let the samples cool more rapidly, higher hardness was obtained from the as-cast samples.

Fig. 7 illustrates the ultimate tensile strength values of as-cast and 1.6 and 2 extruded Al–Mg and Al–Si alloys. The strength of the 1.6 extruded Al–Mg alloy increased by 56% and the strength of the 2 extruded Al–Mg alloy increased 73% in comparison to the strength of the homogeneous as-cast Al–Mg alloy. The strength of the alloy extruded at the ratio of was 11% higher compared to the strength of the alloy extruded at the ratio of 1.6. Similarly, the strength of the 1.6 extruded Al–Si alloy increased by 14% and the strength of the 2 extruded Al–Si alloy increased by 43% in comparison to the strength of the homogenised as-cast Al–Si alloy. The strength of the 2 extruded Al–Mg alloy was 11% higher than the strength of the 1.6 extruded Al–Mg alloy, while the strength of the 2 extruded Al–Si alloy was 25% higher compared to the strength of the 1.6 extruded Al–Si alloy. That is because homogenisation increases in material structure as the ratio of extrusion increases [33,37,38]. It is likely to say that the ability of re-crystallisation increases as the rate of deformation increases in the materials by deforming materials at 350 °C above the re-crystallisation temperature for aluminium alloys [41].

The curves in Fig. 8 illustrate the weight loss variation depending on sliding distance in Al–Mg and Al–Si alloys, extruded at two different ratios, under 10 N, 20 N and 30 N loads. Weight loss increases linearly with increasing sliding distance. The gradients illustrated in Fig. 9 are identified as the rate of wear, and extrusion is evaluated together with the applied force in order to analyse the wear effect (Fig. 9). As can be seen in Fig. 9, as the load applied increases for the specimens with low rate of extrusion, the rate of wear decreases in Al–Si alloys while it increases in Al–Mg alloys. At greater loads, the ductility of Al–Mg alloys is low (Fig. 7B); therefore, they show brittle behaviour, which increases the rate of wear. The rate of wear in highly extruded Al–Mg and Al–Si alloys is very close to each other depending on the applied load. Even though the hardness of both Al–Mg and Al–Si alloys increases with the increase in the rate of extrusion, it causes ductility to decrease in Al–Si alloys and a similarity between the rate of wear of Al–Si alloys and Al–Mg alloys under higher loads [42].

Fig. 9 illustrates the wear rate-load curves under the loads of 10 N, 20 N and 30 N for Al–Si and Al–Mg alloys with two different extrusion ratios. As is seen from the curves, Al–Mg alloys exhibit brittle behaviour due to their low ductility. This causes extensive wear loss in this alloy at high loads (Fig. 8C).

Fig. 10 illustrates SEM images and energy-dispersive X-ray spectroscopy (EDS) analyses for the worn Al–Si and Al–Mg alloys, extruded at two different rates. The worn surface images show that the wear is adhesive and material is transferred from the counter material. EDS analyses show the traces of Al, Si, Fe, Cr and O peaks on the worn surface. While Al, Si and Mg elements were already present in the worn material, Fe and Cr were transferred over from the counter material [8,40]. EDS analyses show an oxygen peak caused by the iron oxide formed as a result of the Fe reacting with the oxygen in the atmosphere [6]. Previous studies state that the formation of iron oxide on the surface decreases the amount of wear [21,39,43–45]. EDS analyses illustrate that oxygen and iron peaks increase together with the increase in the ratio of extrusion, ultimately forming a thicker iron oxide layer on the worn surface [3,40]. It proves that an alloy extruded at a high ratio will have a higher level of wear resistance. As the iron oxide formed on the worn surface acts as a lubricant during the wear, it increases the wear resistance [6,21,40,44]. Depending on the weight loss-wear distance curves illustrated in Fig. 8, it is likely to say that the weight loss values in the Al–Mg alloy are greater in comparison to the weight loss values in the Al–Si alloy. It indicates that alloys containing less than 5% Mg have lower wear resistance [21]. Various studies in the literature show that adding silicon to aluminium alloys increases their wear resistance [39,8].

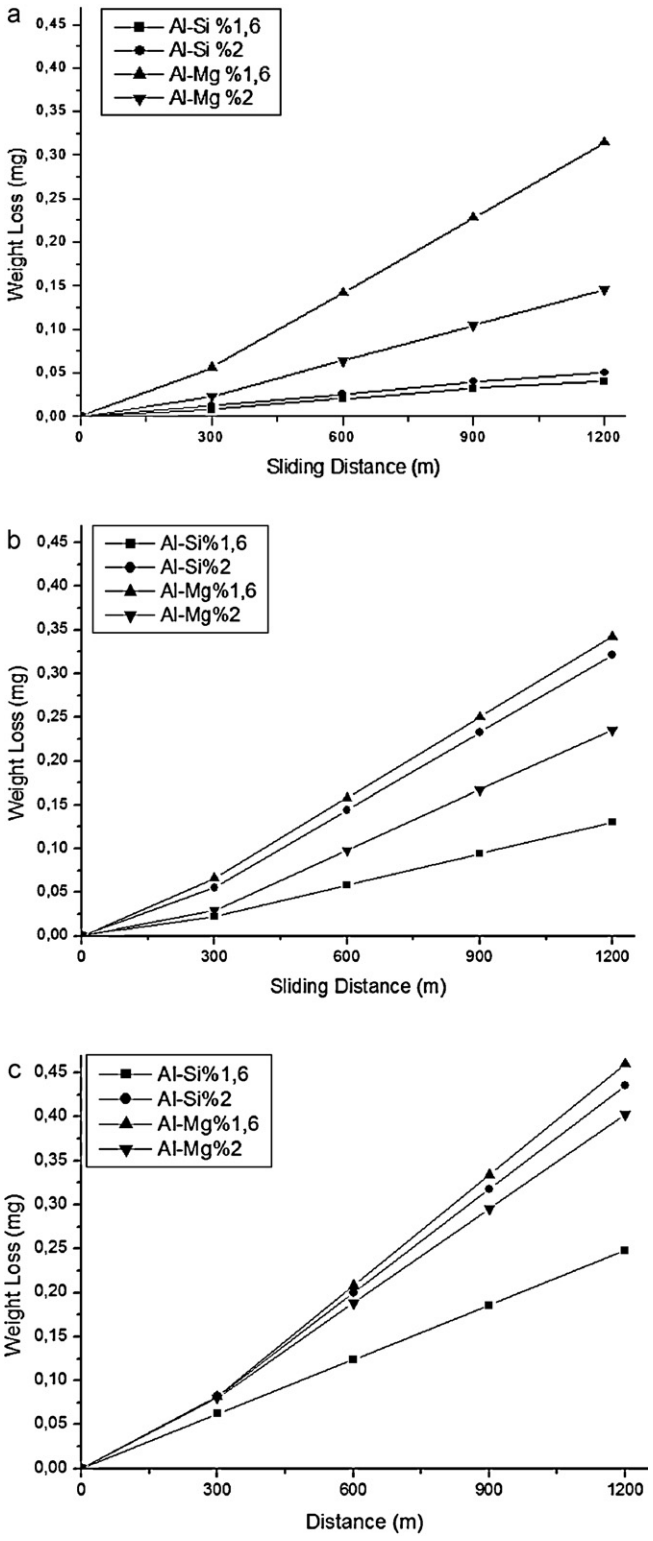

Fig. 8. The weight loss values for Al–Si and Al–Mg alloys extruded at two different ratios under loads of (A) 10 N, (B) 20 N and (C) 30 N.

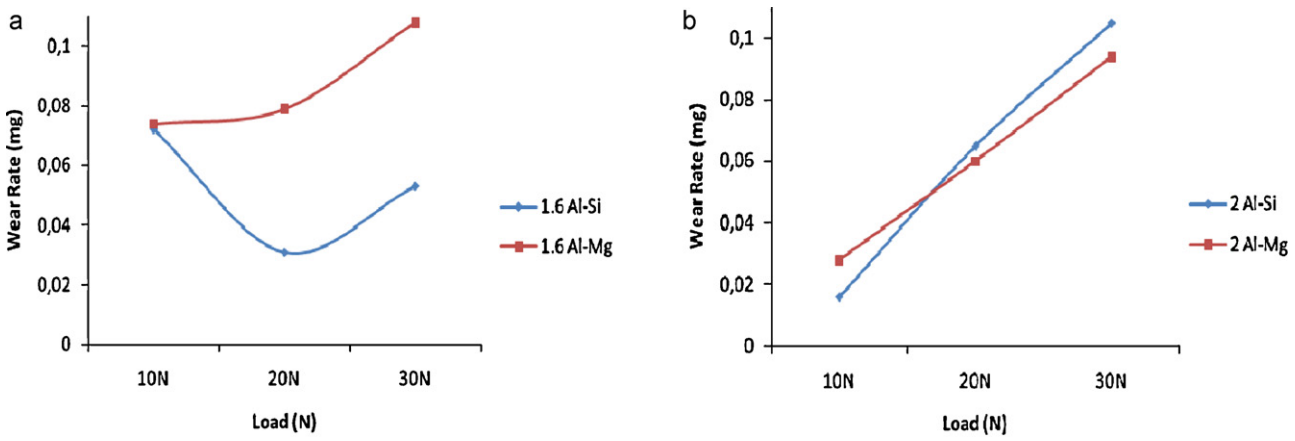

Fig. 9. The wear rate-load graphs under loads of 10 N, 20 N and 30 N for Al–Si and Al–Mg alloys with (A) 1.6 extrusion ratio and (B) 2 extrusion ratio.

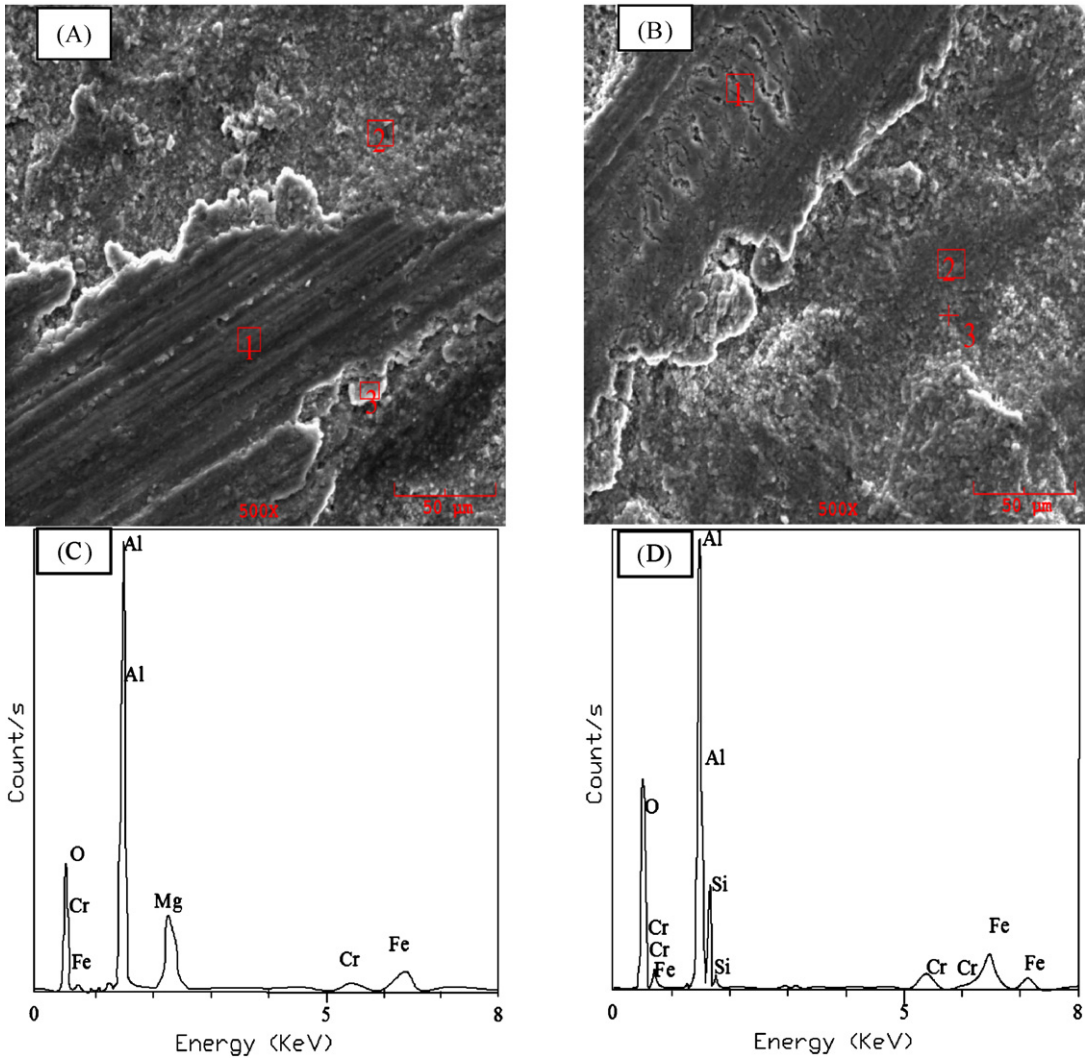

Fig. 10. SEM and EDS analyses for extrudates of extrusion ratio 2: (A) Al–Mg and (B) Al–Si.

4. Conclusions

In this study, Al–Si and Al–Mg alloys were initially die cast and then subjected to hot extrusion at 350 °C. The ratios of extrusion were 1.6 and 2. As a conclusion, it is likely to say that ultimate tensile strength and ductility of the extruded materials were improved. There was a change in the wear behaviour of the alloys, depending on the extrusion ratio and, therefore, in the ductility and ultimate tensile strength. In general, the wear rate increased as ductility decreased.

Wear losses of the Al–Mg alloy were found to be more than those of the Al–Si alloy. The extrusion ratio was also found to influence

the wear losses. 1.6 extruded Al–Mg alloy encountered more wear loss than 2 extruded Al–Mg.

The microstructural observation revealed that the grains were elongated along the extrusion direction. Accordingly, equiaxed grain structure was observed when the microstructure was examined in perpendicular to the extrusion direction. The grains of Al–Si alloy were elongated more than those of Al–Mg alloy.

Acknowledgements

We extend our special thanks to Associate Prof. Dr. Dursun Özyurek, Associate Prof. Dr. Hayrettin Ahlatci, Associate Prof. Dr. İbrahim Çiftci and Karabük University, Faculty of Technical Education for providing great support for us in terms of laboratory equipment and technical expertise.

References

[1] K.G. Satyanarayana, R.M. Pillai, B.C. Pai, M. Kestursatya, P.K. Rohatgi, J.K. Kim, Proc. of the Third Int. Conf., Adv. in Comp. Mat., Bangalore, 2000, pp. 753–763.
[2] C.S. Ramesh, A.R. Anwar Khan, N. Ravikumar, P. Savanprabhu, Wear 259 (2005) 602–608.
[3] R.K. Uyyuru, M.K. Surappa, S. Brusethaugc, Tribol. Int. 40 (2007) 365–373.
[4] Md. Aminul Islam, Z.N. Farhat, Tribol. Int. 44 (2011) 498–504.
[5] T.H. Lee, S.J. Hong, J. Alloys Compd. 487 (2009) 218–224.
[6] K.T. Cho, S. Yoo, K.M. Lim, H.S. Kim, W.B. Lee, J. Alloys Compd. 509 (2011) 265–270.
[7] S.A. Kori, T.M. Chandrashekharaiah, Wear 263 (2007) 745–755.
[8] D.E. Lozano, R.D. Mercado-Solis, A.J. Perez, J. Talamantes, F. Morales, M.A.L. Hernandez-Rodriguez, Wear 267 (2009) 545–549.
[9] S.B. Hassan, V.S. Aigbodion, J. Alloys Compd. 486 (2009) 309–314.
[10] A. Gaber, N. Afify, M.S. Mostafa, Gh. Abbady, J. Alloys Compd. 477 (2009) 295–300.
[11] S.K. Panigrahi, R. Jayaganthan, J. Alloys Compd. 470 (2009) 285–288.
[12] J. Bai, Y. Sun, F. Xue, S. Xue, J. Qiang, T. Zhu, J. Alloys Compd. 437 (2007) 247–253.
[13] A.A. Luo, M.R. Balogh, B.R. Powell, Metall. Mater. Trans. A 33 (2002) 567–574.
[14] Y. Chino, M. Kobata, H. Iwasaki, M. Mabuchi, Mater. Trans. 43 (2002) 2643–2646.
[15] K. Ozturk, Y. Zhong, A.A. Luo, Z.K. Liu, JOM 55 (2003) A40–A44.
[16] K. Hirai, H. Somekawa, Y. Takigawa, K. Higashi, Mater. Sci. Eng. A 403 (2005) 276–280.
[17] H. Akgül, ZKÜ FBE MK ABD, M.Sc. Thesis, Karabük, 2007.
[18] M. Gupta, S.J. Ling, J. Alloys Compd. 287 (1999) 284.
[19] K. Laue, H. Stenger, Extrusion Processes, Machinery, Tooling (A.F. Castle, G. Lang, Trans.), American Soc. for Met., 1981.
[20] P.K. Saha, Alüminyum Ekstrüzyon Teknolojisi (E. Keleşoğlu, Y. Erarslan, Trans.), ASM International The Materials Information Society, Ege Basımevi, İstanbul, 2005.
[21] H. Ahlatçı, Mater. Lett. 62 (20) (2008) 3490–3492.
[22] I. Özdemir, M. Toparlı, J. Compos. Mater. 37 (20) (2003) 1839–1850.
[23] U. Cocen, K. Onel, Comput. Sci. Technol. 62 (2002) 275–282.
[24] J. An, Y.B. Liu, Y. Lu, Q.Y. Zhang, C. Dong, Wear 256 (2004) 374–385.
[25] Y. Chen, Q. Wang, J. Peng, C. Zhai, W. Ding, J. Mater. Process. Technol. 182 (2007) 281–285.
[26] M. Richert, J. Richert, J. ZasadziNski, S. Hawryłkiewicz, J. Długopolski, Mater. Chem. Phys. 81 (2003) 528–530.
[27] O.N. Senkov, S.V. Senkova, J.M. Scott, D.B. Miracle, Mater. Sci. Eng. A 393 (2005) 12–21.
[28] R.Y. Lapovok, M.R. Barnett, C.H.J. Davies, J. Mater. Process. Technol. 146 (2004) 408–414.
[29] A.A. Milenin, S. Berski, G. Banaszek, H. Dyja, J. Mater. Process. Technol. 157–158 (2004) 208–212.
[30] S. Kaneko, K. Murakami, T. Sakai, Mater. Sci. Eng. A 500 (2009) 8–15.
[31] W. Tang, S. Huang, S. Zhang, D. Li, Y. Peng, J. Mater. Process. Technol. 211 (7) (2011) 1203–1209.
[32] X. Duan, T. Sheppard, Mater. Sci. Eng. A 351 (1–2) (2003) 282–292.
[33] M. Erdoğan, Mat. Sci. and Eng. Mat., vol. 1, Nobel Publishing House, Ankara, 2001.
[34] G. Ran, J-E. Zhou, S. Xi, P. Li, J. Alloys Compd. 419 (2006) 66–70.
[35] H. Watanabe, M. Yamaguchi, Y. Takigawa, K. Higashi, Mater. Sci. Eng. A 454–455 (2007) 384–388.
[36] H. ÜN, PAÜ İnşaat Müh Böl. Malz. Bil. Ders Notu, 2007.
[37] C. Zubizarreta, I. Arribas, S. Gimenéz, I. Iturriza, Pow. Met. World Cong., Paris, 2006, pp. 718–719, C02-02-2.
[38] D.W. Suh, S.Y. Lee, K.H. Lee, S.K. Lim, K.H. Oh, J. Mater. Process. Technol. 155–156 (2004) 1330–1336.
[39] M. Elmadagli, T. Perry, A.T. Alpas, Wear 262 (2007) 79–92.
[40] H. Ahlatcı, E. Candan, H. Cimenoglu, Met. Mater. Trans. A 35 (2004) 2127–2141.
[41] J. Corrochano, J.C. Walker, M. Lieblich, J. Ibánez, W.M. Rainforth, Wear 270 (2011) 658–665.
[42] U. Ozsarac, F. Findik, M. Durman, Mater. Des. 28 (2007) 345–350.
[43] G. Sabatini, L. Ceschini, C. Martini, J.A. Williams, I.M. Hutchings, Mater. Des. 31 (2010) 816–828.
[44] J. An, C. Dong, Q.Y. Zhang, Tribol. Int. 36 (2003) 25–34.
[45] J.K. Thompson, W. Li, S.J. Park, A. Antonyraj, R.M. German, F. Findik, Powder Metallurgy 52 (3) (2009) 238–243.